

Water-in-Water Emulsions Stabilized by Nanoplates

Mark Vis,[†] Joeri Opdam,[†] Ingo S. J. van 't Oor,[†] Giuseppe Soligno,[‡] René van Roij,[‡] R. Hans Tromp,^{†,§} and Ben H. Ern ^{*,†}

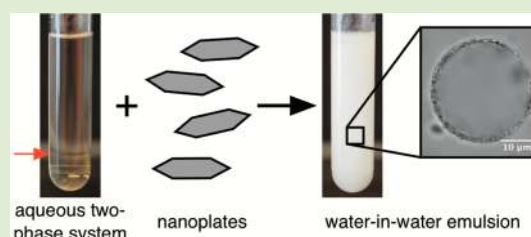
[†]Van 't Hoff Laboratory for Physical and Colloid Chemistry, Debye Institute for Nanomaterials Science, Utrecht University, Padualaan 8, 3584 CH Utrecht, The Netherlands

[‡]Institute for Theoretical Physics, Center for Extreme Matter and Emergent Phenomena, Utrecht University, Leuvenlaan 4, 3584 CE Utrecht, The Netherlands

[§]NIZO food research, Kernhemseweg 2, 6718 ZB Ede, The Netherlands

Supporting Information

ABSTRACT: Ultrathin plate-like colloidal particles are effective candidates for Pickering stabilization of water-in-water emulsions, a stabilization that is complicated by the thickness and ultralow tension of the water–water interface. Plate-like particles have the advantage of blocking much of the interface while simultaneously having a low mass. Additionally, the amount of blocked interface is practically independent of the equilibrium contact angle θ at which the water–water interface contacts the nanoplates. As a result, the adsorption of nanoplates is stronger than for spheres with the same maximal cross section, except if $\theta = 90^\circ$.



Dairy products and many other foods are emulsions: oil droplets in water or water droplets in oil.¹ In principle, emulsions can also be made without oil, by dispersing an aqueous polymer solution in a second, immiscible aqueous polymer solution.^{2–7} This is of interest for the development of novel cosmetics, pharmaceuticals, or low-calorie foods based on oil-free emulsions. However, it is a challenge to find effective stabilizers for such water-in-water emulsions, due to the large thickness^{8–10} and corresponding ultralow tension^{11–14} of the “water–water interface”. Here, we reveal that Pickering stabilization can be realized by ultrathin submicrometer nanoplates. The success of this approach will be explained on the basis of experiments and theory.

To understand why stabilizing water-in-water emulsions is so difficult, it is important to know about the physical chemistry of the water–water interface. This phase boundary is created when an aqueous solution of two different polymers is concentrated to such an extent that it spontaneously demixes into two coexisting polymer solutions. Both phases typically contain 90% water, and the interface is permeable to water and small ions.^{15,16} To the naked eye, the macroscopic interface looks sharp (Figure 1a), but on the molecular scale (Figure 1b), it is much thicker than the interface between two molecular liquids such as water and oil. The relative concentration of each polymer varies gradually from the bulk value in the first phase to the bulk value in the second phase across distances of tens of nm (Figure 1c), depending on how close the polymer concentrations are to the critical point of demixing.^{8–10} This is a much larger distance than, for instance, the ~ 0.3 nm size of a water molecule. In the interfacial zone, the total polymer concentration features a local minimum, since the repulsion

between the two different types of polymers resists interpenetration (Figure 1d). Due to the weak interfacial gradients, the energy per unit area associated with creating the interface is extremely low, 3–6 orders of magnitude lower than the tension of a water–oil interface. The large interfacial thickness and the ultralow interfacial tension complicate the search for effective stabilizers of water-in-water emulsions.

The aqueous two-phase system that we set out to emulsify in our experiments contains 5–9% dextran and 3–5% cold-water fish gelatin by mass. Dextran is a polysaccharide, and cold-water fish gelatin is a protein with almost the same amino acid composition as gelatin used in the kitchen; however, it must be cooled below 10 °C before it starts to form a gel, and as a result, our system remains liquid at room temperature. Our biopolymers each have a molecular mass of 100 kDa and a high polydispersity. Dextran is uncharged and, also, gelatin is practically uncharged under our conditions of neutral pH and ~ 5 mM salt.^{16–18} Demixing of our aqueous solutions of dextran and gelatin occurs above a critical mass fraction of about 3% of each polymer (Figure 1e). In our experiments, the interfacial tension is ~ 4 $\mu\text{N/m}$ (Figure 1f), a factor $\sim 10^4$ lower than for a typical water–oil interface.^{19,20}

In systems with water and oil, emulsion droplets are usually stabilized by interfacial adsorption of either molecular surfactants or colloidal particles. A surfactant molecule of a few nm in length will adsorb at the water–oil interface when one of its extremities has a strong affinity for water and the

Received: July 14, 2015

Accepted: August 17, 2015

Published: September 2, 2015

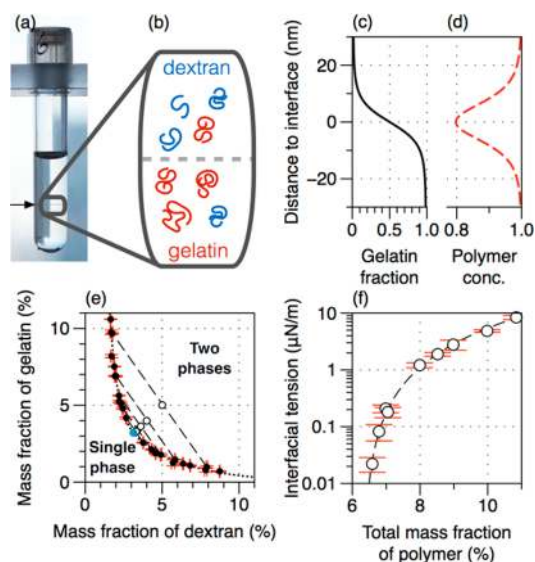


Figure 1. (a) Photograph and (b) schematic of a 1.2 cm wide tube with 6.0% dextran and 6.0% gelatin in water. The water–water interface is indicated by an arrow. (c) Polymer fraction of gelatin and (d) relative total polymer concentration calculated in the phase boundary zone for our chemical system via the method in ref 9. (e) Experimental demixing phase diagram of dextran and gelatin in water.¹⁷ (f) Interfacial tension vs total polymer concentration.

other extremity prefers oil. However, the thickness of water–water interfaces prevents the use of such small molecular surfactants, which cannot straddle the whole interfacial zone. Only larger purpose-designed block copolymers can be successful macromolecular stabilizers of water-in-water emulsions, as demonstrated by Buzza et al.⁶

The second option, using colloidal particles as surfactants, is commonly called Pickering stabilization^{19,20} and finds application in the preparation of colloidosomes.^{2,21} The adsorption of colloids at the liquid–liquid interface prevents coalescence of liquid droplets by keeping their inner liquids sufficiently far apart, and even partial coverage of the droplets by colloids can suffice for good stabilization.^{22,23} When the colloidal particles have a uniform surface chemistry, the adsorption energy is at most equal to $\gamma\sigma$,²³ with γ the liquid–liquid interfacial tension and σ the cross sectional area of a colloidal particle. The ultralow tension of the water–water interface thus gives rise to a relatively weak adsorption that only exceeds the thermal energy scale $k_B T \approx 4 \times 10^{-21}$ J if σ is sufficiently large. Setting the adsorption energy for strong adsorption to $20 k_B T$ requires spherical particles with a diameter of only 1.6 nm for a typical water–oil interface with a tension of 40 mN/m (if the wetting angle is 90°), but the particle diameter must be at least 160 nm for our water–water interface with $\gamma \approx 4 \mu\text{N/m}$. Adsorbed colloidal particles of 160 nm are likely to result in rapid sedimentation of the droplets and therefore poor emulsion stability, except if the mass density of the colloids closely matches that of the liquid. Our approach here is to use nanoplates, because their buoyant mass is much lower than that of spheres of the same density and cross section.

Numerical calculations based on the capillary deformation of an initially flat water–water interface by the adsorption of nanoplates are shown in Figure 2 at a variety of orientations and positions with respect to the interface. The employed numerical method stems from Soligno et al.²⁴ and is summarized in the Supporting Information (SI), Theoretical

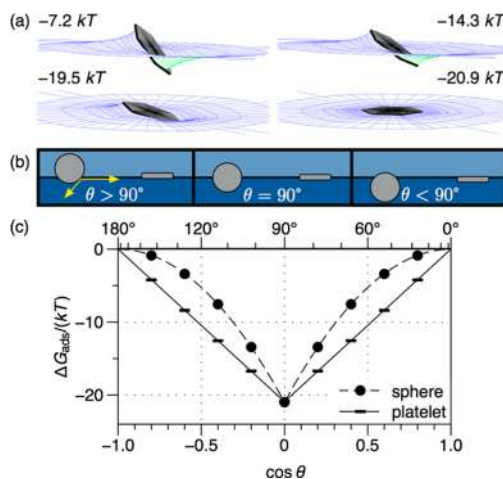


Figure 2. Numerical calculations of the adsorption energy of nanoplates with an effective diameter of 167 nm at the water–water interface, $\gamma = 4 \mu\text{N/m}$. (a) Strengthening of the adsorption as a nanoplate reorients itself to lie flat in the liquid–liquid interface ($\theta = 90^\circ$). (b) Schematic of how the contact angle has little effect on the blocked area of liquid–liquid interface in the case of a platelet, as opposed to the case of a sphere. (c) Adsorption energy of platelets and spheres as a function of the wetting angle θ . The symbols are from numerical simulations, and the curves are from eq 1 (sphere) and eq 2 (platelet).

methods, together with SI, Figures S4–S10. The calculations here are for hexagonal nanoplates, but results are similar for discs. A first conclusion is that nanoplates prefer to lie flat along the water–water interface (Figure 2a), minimizing its surface area and energy. A second conclusion is that the thin rim of the particles accommodates most contact angles without any substantial change in the blocked area of the water–water interface (Figure 2b).²⁵ As a result, the adsorption energy is the same as for spheres with the same cross sectional area only at a contact angle of 90° ; at other contact angles, the adsorption of a sphere becomes weaker than that of a platelet (Figure 2c). Nevertheless, the adsorption of the nanoplates still depends on the contact angle, because a deviation of the contact angle from 90° at fixed tension of the liquid–liquid interface implies a change in the tensions of the two solid–liquid interfaces. Whereas the adsorption energy of a sphere of diameter d is given by²⁰

$$\Delta G_{\text{ads}}(\text{sphere}) = -(\pi/4)d^2\gamma(1 - \cos \theta)^2 \quad (1)$$

we find from analytical theory (SI, equation S9) that for a nanoplate of negligible thickness, it is given by

$$\Delta G_{\text{ads}}(\text{platelet}) = -(\pi/4)d^2\gamma(1 - \cos \theta) \quad (2)$$

Adsorption energy thus scales linearly with $(1 - \cos \theta)$ in the case of platelets, instead of quadratically for spheres.

The effectiveness of nanoplates as stabilizers of water-in-water emulsions is illustrated by our experimental results in Figure 3. Without stabilizer, the solution demixes into a dextran-rich upper phase and a gelatin-rich lower phase (Figure 3a). After mixing with hexagonal gibbsite plates with an effective diameter of ~ 170 nm and a thickness of ~ 7 nm, an emulsion is obtained that remains stable for weeks (Figure 3b). Larger, ~ 700 nm sized, gibbsite plates with a thickness of ~ 35 nm are less effective stabilizers (Figure 3c), which probably is related to their larger buoyant mass.

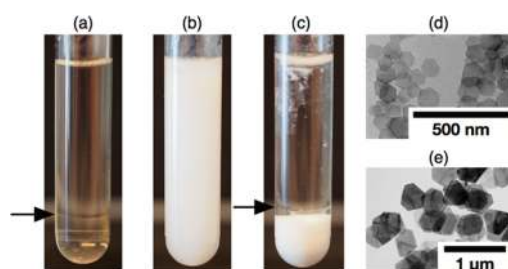


Figure 3. Emulsification of 9% dextran and 3% nongelling fish gelatin in water using gibbsite nanoplates as a Pickering stabilizer. (a) No nanoplates. (b) Stable emulsion obtained with gibbsite nanoplates 167 ± 30 nm wide and 6.6 ± 1.1 nm thick. (c) Partial emulsification obtained with larger gibbsite nanoplates, 694 ± 45 nm wide and 30 to 40 nm thick. Electron micrographs of (d) 167 and (e) 694 nm nanoplates. The arrows in (a) and (c) indicate the water–water interface. The pictures in (a)–(c) were taken 2 weeks after sample preparation by vortex mixing.

The thermodynamic tendency of colloidal particles to sediment is characterized by the so-called sedimentation length $L_g = k_B T / (\Delta m g)$, where Δm is the buoyant mass of a colloidal particle and g is the acceleration due to gravity.²⁶ The sedimentation length of the 700 nm platelets is merely 0.02 mm, as compared to 2 mm for the 170 nm platelets. $L_g = 2$ mm for the smaller platelets is still much smaller than the size of the glass sample tube, which raises the question why the small platelets stabilize emulsions so well. We find an explanation in the microscopic structure of the emulsion (Figure 4).

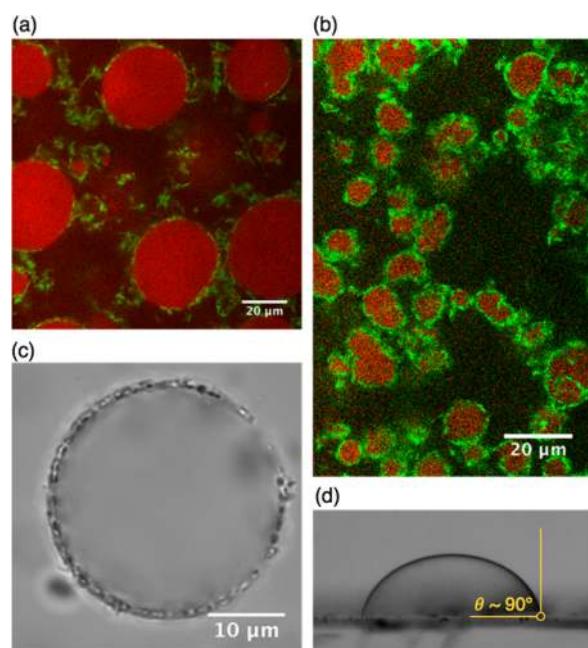


Figure 4. Confocal microscopy of an emulsion of 9% dextran and 3% gelatin stabilized by (a) 0.4% and (b) 1% of 170 nm sized gibbsite platelets. The interface is highlighted green due to FITC–dextran; the gelatin-rich droplets are stained red with Rhodamine B.¹⁰ (c) Gibbsite plates (700 nm) at the surface of a dextran-rich droplet in an emulsion of 5% dextran and 5% nongelling fish gelatin. (d) Gelatin-rich droplet ($1 \mu\text{L}$) surrounded by dextran-rich continuous phase on a gibbsite-covered glass substrate, sharing a three-phase contact angle close to 90° (advancing interface, see SI, movies S6–S9).

With the small gibbsite platelets (Figure 4a,b), the water–water interface is presumably covered in a relatively uniform manner, as evidenced by the loss of spherical shape of the droplet upon increasing the gibbsite concentration, which indicates saturation of the surface coverage. The larger platelets in Figure 4c are clearly found at the surface of the droplet and exhibit Brownian motion, lying flat as expected but with a higher concentration at the bottom than at the top of the droplet (SI, movies S1–S5). The larger platelets not only render the droplets heavy, but also settle to the bottom of each droplet, leaving it less well stabilized on top. The smaller platelets effectively stabilize the droplets, which do not settle, because a high fraction of the sample volume is filled with droplets and because some bridging of the droplets by gibbsite occurs. The system may possibly form a loose gel, but it still flows as a liquid upon tilting of the sample tube.

A fair question concerns the specificity of gibbsite, a synthetic clay composed of crystalline aluminum hydroxide, as a stabilizer of our water-in-water emulsions. Emulsions based on water and oil have been stabilized by clay(-like) particles, and interactions between the platelets influence the structure and stability of the emulsions.^{27–29} In our present study at neutral pH and ~ 5 mM ionic strength, we can neglect electrical interactions between the nanoplates and the water–water interface, which is practically uncharged.¹⁶ Chemical affinity between gibbsite and both types of polymer is, however, indicated by two types of observations. The effective hydrodynamic size of our gibbsite nanoplates dispersed in water increases upon addition of low concentrations of dextran or gelatin (SI, Dynamic light scattering results). Further evidence is given by the wetting angle close to 90° for a gelatin-rich droplet in a dextran-rich continuous phase at a gibbsite-covered glass substrate (Figure 4d and SI, movies S6–S9). The lack of a clear preference of gibbsite nanoplates for gelatin- or dextran-rich phase is in line with the observation that they can stabilize both gelatin-rich droplets in dextran-rich continuous phase (Figures 3b and 4a,b) and dextran-rich droplets in gelatin-rich continuous bottom phase (Figures 3c and 4c).

Another question concerns the structure of the interface. In our theoretical calculations (Figure 2), we treat the water–water interface as abrupt, ignoring its thickness. We speculate that, in reality, the nanoplates straddle much of the central interfacial zone, where the total polymer concentration is lowest (Figure 1c). The molecular details remain a question for future study. Nevertheless, it seems clear that chemical affinity of the platelets for both types of polymer is a prerequisite to obtain stable water-in-water Pickering emulsions.

In conclusion, nanoplates, instead of nanospheres, are well suited for the Pickering stabilization of water-in-water emulsions. They block a relatively large area of the water–water interface without causing the emulsion droplets to become so heavy that the emulsion becomes unstable. Moreover, the adsorption of nanoplates is much less sensitive to the three-phase wetting angle than spheres, allowing application in a greater range of chemically distinct interfaces. One of the current challenges is to find suitable food-grade or pharma-grade alternatives for gibbsite, for instance plate-like particles made from protein, polysaccharide, or fat. Our main contribution here is to provide useful physical insights to guide the development of novel oil-free emulsions, with a view to application in cosmetics, pharmaceuticals, or low-calorie foods.

METHODS

Biopolymers dextran (Sigma-Aldrich, from *Leuconostoc* spp., average molar mass 100 kDa) and gelatin (fish gelatin type A; average molar mass 100 kDa; gelling temperature 8–10 °C; from Norland Products, kindly provided by FIB Foods, Harderwijk, The Netherlands) were dissolved in Milli-Q water, the gelatin solution having been heated to 60 °C before the experiments were performed at room temperature (20 °C). The pH was 6.2 and the salt concentration approximately 5 mM, as deduced from electric conductivity measurements. Polymer solutions were mixed with colloidal dispersions of gibbsite platelets, synthesized by hydrothermal treatment of aluminum alkoxides in acidic environment^{30,31} and with dimensions characterized by electron microscopy and atomic force microscopy. Emulsions were imaged by confocal microscopy, and the dyes Rhodamine B and fluorescein isothiocyanate–dextran were added to color the gelatin-rich phase and the liquid–liquid interface, respectively.¹⁰ Interfacial tensions were calculated from the precise densities of the two phases and microscopic registration of the shape of the water–water interface after full phase separation; that shape results from a balance between gravitational energy and the Laplace pressure difference across the curved interface. Dynamic light scattering was performed using a Malvern Zetasizer Nano ZS on dispersions whose viscosity had been measured using an Anton Paar MCR-300 rheometer. Further details are provided in the [Supporting Information](#).

ASSOCIATED CONTENT

Supporting Information

Movies with optical micrographs showing 3D scans of gibbsite-stabilized emulsions and time-dependence of the contact angle measurements; details of the sample preparations; details of the determination of ultralow interfacial tensions from optical micrographs of capillary rise at a vertical wall; methods of the contact angle measurements; methods and results of the DLS experiments; methods and additional results of the geometrical calculations of nanoplate interaction with the water–water interface. The Supporting Information is available free of charge on the [ACS Publications website](#) at DOI: [10.1021/acsmacrolett.5b00480](https://doi.org/10.1021/acsmacrolett.5b00480).

Description of movies; experimental and theoretical details ([PDF](#))

Movie S1 ([AVI](#))

Movie S2 ([AVI](#))

Movie S3 ([AVI](#))

Movie S4 ([AVI](#))

Movie S5 ([AVI](#))

Movie S6 ([AVI](#))

Movie S7 ([AVI](#))

Movie S8 ([AVI](#))

Movie S9 ([AVI](#))

AUTHOR INFORMATION

Corresponding Author

*E-mail: b.h.erne@uu.nl.

Notes

The authors declare no competing financial interest.

ACKNOWLEDGMENTS

M.V., R.H.T., and B.H.E. acknowledge financial support from The Netherlands Organisation for Scientific Research (NWO). G.S. and R.R. acknowledge financial support by a NWO Vici Grant and by the Marie Curie Initial Training Network “Soft Matter at Aqueous Interfaces” (SOMATAI). This work is part of the D-ITP consortium, a program of NWO funded by the Dutch Ministry of Education, Culture, and Science (OCW).

The authors thank Vincent Peters for the interfacial tension measurements, Dominique Thies-Weesie for the viscosity measurements, Elleke van Harten for providing the large gibbsite platelets, Sonja Castillo for the SEM micrographs, Jos van Rijssel for assistance with the contact angle measurements, Edgar Blokhuis for useful discussions, and John Kelly for critical reading of the manuscript.

REFERENCES

- (1) McGee, H. *McGee on Food and Cooking: An Encyclopedia of Kitchen Science, History, and Culture*; Hodder & Stoughton: London, 2004.
- (2) Poortinga, A. T. *Langmuir* **2008**, *24*, 1644–1647.
- (3) Firoozmand, H.; Murray, B. S.; Dickinson, E. *Langmuir* **2009**, *25*, 1300–1305.
- (4) Balakrishnan, G.; Nicolai, T.; Benyahia, L.; Durand, D. *Langmuir* **2012**, *28*, 5921–5926.
- (5) Nguyen, B. T.; Nicolai, T.; Benyahia, L. *Langmuir* **2013**, *29*, 10658–10664.
- (6) Buzza, D. M. A.; Fletcher, P. D. I.; Georgiou, T. K.; Ghasdian, N. *Langmuir* **2013**, *29*, 14804–14814.
- (7) Nguyen, B. T.; Wang, W.; Saunders, B. R.; Benyahia, L.; Nicolai, T. *Langmuir* **2015**, *31*, 3605–3611.
- (8) Broseta, D.; Leibler, L.; Kaddour, L. O.; Strazielle, C. J. *J. Chem. Phys.* **1987**, *87*, 7248.
- (9) Tromp, R. H.; Blokhuis, E. M. *Macromolecules* **2013**, *46*, 3639–3647.
- (10) Tromp, R. H.; Vis, M.; Ern , B. H.; Blokhuis, E. M. *J. Phys.: Condens. Matter* **2014**, *26*, 464101.
- (11) Ryden, J.; Albertsson, P.-Å. *J. Colloid Interface Sci.* **1971**, *37*, 219–222.
- (12) Ding, P.; Wolf, B.; Frith, W. J.; Clark, A. H.; Norton, I. T.; Pacek, A. W. *J. Colloid Interface Sci.* **2002**, *253*, 367–376.
- (13) Simeone, M.; Alfani, A.; Guido, S. *Food Hydrocolloids* **2004**, *18*, 463–470.
- (14) Antonov, Y. A.; van Puyvelde, P.; Moldenaers, P. *Int. J. Biol. Macromol.* **2004**, *34*, 29–35.
- (15) Scholten, E.; Sagis, L. M. C.; van der Linden, E. *Biomacromolecules* **2006**, *7*, 2224–2229.
- (16) Vis, M.; Peters, V. F. D.; Tromp, R. H.; Ern , B. H. *Langmuir* **2014**, *30*, 5755–5762.
- (17) Vis, M.; Peters, V. F. D.; Ern , B. H.; Tromp, R. H. *Macromolecules* **2015**, *48*, 2819–2828.
- (18) Vis, M.; Peters, V. F. D.; Blokhuis, E. M.; Lekkerkerker, H. N. W.; Ern , B. H.; Tromp, R. H. *Phys. Rev. Lett.* **2015**, *115*, 078303.
- (19) Binks, B. P. *Curr. Opin. Colloid Interface Sci.* **2002**, *7*, 21–41.
- (20) Binks, B. P.; Horozov, T. S. *Colloidal Particles at Liquid Interfaces*; Cambridge University Press: New York, 2006.
- (21) Dinsmore, A. D.; Hsu, M. F.; Nikolaidis, M. G.; Marquez, M.; Bausch, A. R.; Weitz, D. A. *Science* **2002**, *298*, 1006–1009.
- (22) Vignati, E.; Piazza, R.; Lockhart, T. P. *Langmuir* **2003**, *19*, 6650–6656.
- (23) Sacanna, S.; Kegel, W. K.; Philipse, A. P. *Phys. Rev. Lett.* **2007**, *98*, 158301–158304.
- (24) Soligno, G.; Dijkstra, M.; van Roij, R. *J. Chem. Phys.* **2014**, *141*, 244702.
- (25) Singh, P.; Joseph, D. D. *J. Fluid Mech.* **2005**, *530*, 31–80.
- (26) Everett, D. H. *Basic Principles of Colloid Science*; Royal Society of Chemistry: Cambridge, 1988.
- (27) Zhang, N.; Zhang, L.; Sun, D. *Langmuir* **2015**, *31*, 4619–4626.
- (28) Guillot, S.; Bergaya, F.; de Azevedo, C.; Warmont, F.; Tranchant, J.-F. *J. Colloid Interface Sci.* **2009**, *333*, S63–S69.
- (29) Whitby, C. P.; Fornasiero, D.; Ralston, J. *J. Colloid Interface Sci.* **2008**, *323*, 410–419.
- (30) Wierenga, A. M.; Lenstra, T. A. J.; Philipse, A. P. *Colloids Surf., A* **1998**, *134*, 359–371.
- (31) Wijnhoven, J. E. G. J. *J. Colloid Interface Sci.* **2005**, *292*, 403–409.